Aggregation Properties of Hyperporphyrins with Hydroxyphenyl Substituents

Giovanna De Luca, Andrea Romeo, and Luigi Monsù Scolaro*

Dipartimento di Chimica Inorganica, Chimica Analitica e Chimica Fisica, and C.I.R.C.M.S.B., Università di Messina, Salita Sperone 31, 98166 Vill. S. Agata, Messina, Italy

Received: March 28, 2006; In Final Form: May 31, 2006

Acidification of tetrakis(4-hydroxyphenyl)porphyrin (THPP) and tetrakis(3,5-dihydroxyphenyl)porphyrin (OHPP) in dichloromethane solutions has been investigated as a function of the nature of the counteranion. These porphyrins exhibit different patterns of behavior, and extended aggregates are formed displaying broad extinction features together with intense components due to resonant light scattering. Especially in the case of haloacids, J-aggregated species are obtained exhibiting large bathochromic shifts both for B- and Q-bands, which extend in the far red region. The optical characteristics of the aggregated and monomeric protonated species are strongly influenced by the nature of the counteranions. A comparison with tetrakis(4-methoxyphenyl)porphyrin (TMPP), which remains always in a monomeric form, demonstrates the key role played by the peripheral hydroxyl groups in stabilizing various porphyrin aggregates.

Introduction

The dependence of the physicochemical properties of porphyrins on their peripheral functionalization has been studied extensively.[1,2] A case in point involves photodynamic therapy (PDT), which is one of the most important applications of this class of chromophores, where various porphyrin derivatives can be used as sensitizers to photoinitiate the destruction of tumor cells.[3,4] One of the requirements for an ideal photosensitizer consists of having a high extinction coefficient at long wavelengths (600−800 nm), where tissue penetration of light is at maximum and photons are still sufficiently energetic to produce singlet oxygen.[5] This requirement is fulfilled by porphyrins bearing hydroxyphenyl substituents at the *meso* positions, these molecules being among the most potent photosensitizers studied.[6−9] Several investigations of the acid−base behavior of hydroxyphenyl-substituted porphyrins (as well as (dimethylamino)phenyl derivatives) have shown the presence of unusually broad and red shifted, or even split, absorption features under various conditions.[10−15] Such molecules have been referred to as *hyperporphyrins*,[2] and the origins of their characteristic spectroscopic features have been identified as charge-transfer processes from the peripheral substituents toward the porphine macrocycle or vice versa.[10,11,16] Normal porphyrin spectra are characterized by the presence of the strongly allowed Soret band in the near-UV and of the less intense (quasi-allowed) Q-bands at longer wavelengths. These features are usually well-described by the four-orbital model proposed by Gouterman et al.[2,17] which is characterized as singlet $\pi-\pi^*$ transitions between the two nearly degenerate HOMOs $a_{1u}(\pi)$ and $a_{2u}(\pi)$ and the two degenerate LUMOs $e_g(\pi^*)$. Mixing of these configurations lifts the degeneracy and leads to the aforementioned bands.[2,17] Hyperporphyrin spectra generally show extra bands in the UV/vis region that cannot be described solely by this model. Three types of hyperporphyrins, mainly metal-coordinated derivatives, have been defined, and an orbital mechanism for the relative spectra has been provided by iterative extended Huckel (IEH) calculations.[2,10,18] The so-called *d-type* hyperporphyrins are characterized by porphyrin-to-metal charge-transfer transitions, while in the *p-type* hyperporphyrins a metal-to-porphyrin charge-transfer transition is operative. Whenever the energies of these transitions are comparable to that of the B band transition, a strong interaction occurs, and as a consequence, a split Soret band is observed.[18] The third type of hyperporphyrin includes the carbon monoxide complex of ferrous cytochrome P-450, in which the remaining axial coordination site is occupied by a cysteinate ligand.[19,20] Hyperporphyrin spectra have also been observed for cytochrome P-450 model compounds involving heme[21−23] and metal complexes of tetraphenylporphyrin[24−26] and octaethylporphyrin,[27,28] having mercaptide groups (RS^-) as axial ligands. In these cases, or in the presence of peripheral amino or hydroxyl substituent groups, lone pair orbitals with the correct symmetry are available for a charge-transfer transition from the donor atom to the porphyrin.[10−16]

To the best of our knowledge, the formation of aggregates, which would also lead to broadened and red-shifted extinction features, has not been reported in the literature for porphyrins functionalized with hydroxyphenyl or aminophenyl groups. Following our interest in the behavior of porphyrins upon acidification in organic solvents, we have already investigated tetraphenylporphyrin (TPP),[29] the three isomers of tetrakis(pyridyl)porphyrin (TpyP),[30] and the tetrabutylammonium salt of tetrakis(4-sulfonatophenyl)porphyrin (TPPS).[31] In the latter two cases, extensive aggregation has been pointed out as a function of the nature of porphyrin and the specific acid. Due to the low dielectric constant of dichloromethane, the formation of strong ion pairs has been suggested as responsible for the observed counteranion-dependent spectroscopic properties. These phenomena also cause the deposition of nano- and mesoscopic structures of the above-mentioned porphyrin derivatives by photodecomposition of chlorinated solvents.[32,33]

In this framework, the behavior of tetrakis(4-hydroxyphenyl)porphyrin and tetrakis(3,5-dihydroxyphenyl)porphyrin (THPP and OHPP, respectively; Figure 1) toward acids in dichloromethane solutions has been investigated as a function of the nature of the acid. We anticipate that extended aggregates are

* To whom correspondence should be addressed. E-mail: lmonsu@unime.it. Phone: +39 090 676 5711. Fax: +39 090 393756.

10.1021/jp0619179 CCC: $33.50
Published on Web 07/04/2006

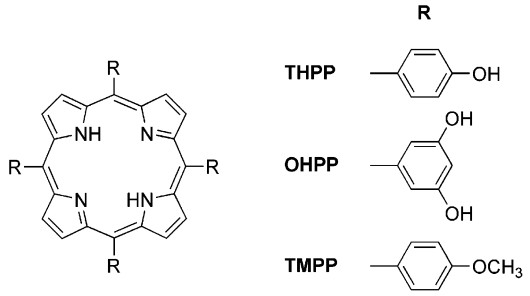

Figure 1. Molecular structures of the investigated porphyrins.

formed displaying broad and red-shifted extinction features together with intense components due to resonant light scattering. As in the case of TpyP isomers and TPPS, the optical characteristics of the aggregated species are strongly affected by the nature of the counteranion, even if it is difficult to recognize a definite trend. A comparison with acidification experiments carried out on tetrakis(4-methoxyphenyl)porphyrin (TMPP) demonstrates the key role of hydroxyl groups in stabilizing various porphyrin aggregates.

Experimental Section

Spectroscopic Methods. UV/vis absorption spectra were measured on a Hewlett-Packard model HP 8453 diode array spectrophotometer. Fluorescence emission and excitation spectra and resonance light-scattering (RLS) experiments were performed on a Jasco model FP-750 spectrofluorometer equipped with a Hamamatsu R928 photomultiplier. For RLS experiments a synchronous scan protocol with a right angle geometry was adopted.[34] No correction has been applied for absorbance of the samples. A UV filter (Hoya glass type UV-34; cutoff, 340 nm) was used in all measurements in order to cut off the UV component of the spectrophotometer lamp, thus avoiding photodecomposition of dichloromethane and the consequent formation of HCl.

Chemicals. *meso*-Tetrakis(4-hydroxyphenyl)porphyrin (THPP) was purchased from Aldrich Chemical Co., while *meso*-tetrakis-(3,5-dihydroxyphenyl)porphyrin (OHPP) was purchased from Tokyo Kasey Kogyo Co., Ltd. *meso*-Tetrakis(4-methoxyphenyl)-porphyrin (TMPP) was prepared and purified according to literature procedures.[35] The purity of these compounds was checked and confirmed through ^{1}H NMR and thin-layer chromatography (TLC). THPP and OHPP were subjected to TLC analyses on neutral alumina plates, using a mixture of methanol/dichloromethane (10/90 and 15/85 v/v, respectively), to which a few drops of triethylamine were added. TMPP was eluted on the same substrate using a mixture of pentane/dichloromethane (40/60 v/v), to which a few drops of triethylamine were added. ^{1}H NMR spectra were recorded on a Bruker AMX-R300 operating at 300.13 MHz, using acetone-d_6 for THPP and OHPP and chloroform-*d* for TMPP. Chemical shifts were referenced downfield to TMS, and data satisfactorily agreed with the literature.[36]

Solutions of these porphyrins were prepared in spectrophotometric grade dichloromethane (Sigma), with the addition of spectrophotometric grade methanol (Aldrich; ~2% v/v) in the case of THPP and OHPP to increase their solubility.[37]

Stock solutions were stored in the dark and used within 1 week of preparation. The range of concentration ($(5-10) \times 10^{-6}$ M) used in our experiments was determined spectrophotometrically using the molar extinction coefficient at the Soret maxima (TMPP, 4.57×10^5 M^{-1} cm^{-1}, $\lambda = 420$ nm; THPP, 4.57×10^5 M^{-1} cm^{-1}, $\lambda = 421$ nm; OHPP, 2.95×10^5 M^{-1} cm^{-1}, $\lambda = 419$ nm).[36]

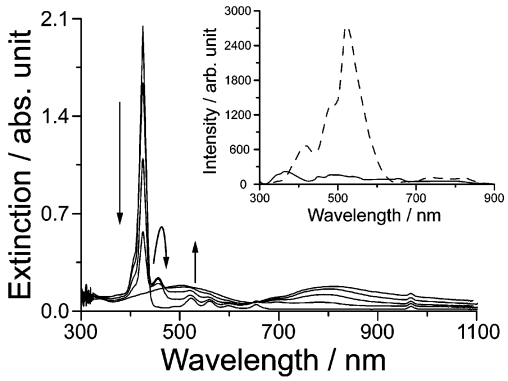

Figure 2. UV/vis spectral changes following the stepwise addition of HCl to a dichloromethane solution of THPP ([THPP] = 4.6 μM). Arrows mark the evolution due to the increase of acid concentration (up to ~150 μM). Inset: RLS of starting (solid line; ×10) and acidified (dashed) solutions.

All the hydrogen halides and trifluoroacetic and trifluoromethanesulfonic acids were of the highest commercial grade available (Aldrich) and were used as received without further purification. Tetrakis[3,5-bis(trifluoromethyl)phenyl]boric acid (HTFPB) was prepared according to a literature procedure.[38] With the hydrogen halides, acidification of the porphyrins solutions was achieved by injecting acid vapors to a prefixed volume of porphyrin stock solution, by using a homemade glass kit connected directly to a reservoir of concentrated acid solution. In the case of the other acids, the additions were done by injecting small amount of neat acid or diluted dichloromethane solutions. The conversion of the porphyrins into the various forms was directly monitored through UV/vis, fluorescence, and RLS spectroscopy.[30,31]

Results and Discussion

Dichloromethane solutions of THPP display a sharp and intense Soret band accompanied by four weaker Q-bands at longer wavelengths in the extinction spectrum. A red fluorescence with two emissions is observed, and the corresponding resonance light scattering (RLS) profile is similar to that of the neat solvent, with a trough due to photon "loss" corresponding to the Soret band. This experimental evidence is in good agreement with a monomeric nature of the free base porphyrin.

As observed for TpyP isomers,[31] addition of HCl vapors to a THPP solution causes extended aggregation. At first, the decrease of the Soret band is accompanied by the appearance of a small feature at 453 nm and by minor changes in the Q-band region (Figure 2). Upon further acid addition, the extinction evolves displaying extremely broad and red-shifted B and Q-bands, having comparable intensities. At the end of the acidification experiment, the fluorescence is totally quenched and the corresponding RLS signal is very intense (Figure 2, inset). These results can be explained by the initial formation of the monomeric diacid derivative $\{H_2THPP(Cl)_2\}$,[39] which aggregates extensively as its concentration increases ($\{H_2THPP(Cl)_2\}_{agg}$).

Extended aggregation is also observed on acidification of THPP solution with HBr or HI. Again in these cases, the presence of two Q-bands in the extinction spectra indicates diprotonation of the porphyrin core. Unlike the chloride system, no intermediate species are detected.

OHPP exhibits essentially the same behavior as THPP toward acidification with the three haloacids, the major difference

TABLE 1: UV/Vis Absorption, Emission, and RLS Features of Species Derived from Porphyrin THPP in the Presence of Various Acids HX in Dichloromethane at 298 K

X^-	species	B-band (λ/nm)	Q-bands (λ/nm)				emission max (λ/nm)		RLS
	THPP	424	519	557	595	651	657	722	
Cl^-	H_2THPP^{2+} [a]	453							
	$H_2THPP^{2+}_{agg}$	500			690	805			522
Br^-	$H_2THPP^{2+}_{agg}$	485			646	761			504
I^-	$H_2THPP^{2+}_{agg}$	493			693	772			514
	$HTHPP^+_{dim}$ [a]	427					609	655	
CF_3COO^-	$H_2THPP^{2+}_{agg}$	481			672	744			491
	H_2THPP^{2+}	448			628	688		736	498
$CF_3SO_3^-$	$H_2THPP^{2+}_{agg}$	474			657	733	678	713	493
	H_2THPP^{2+}	452			646	714		749	493
$TFPB^-$	H_2THPP^{2+}	455			644	707		759	

[a] Intermediate species.

TABLE 2: UV/Vis Absorption, Emission, and RLS Features of Species Derived from Porphyrin OHPP in the Presence of Various Acids HX in Dichloromethane at 298 K

X^-	species	B-band (λ/nm)	Q-bands (λ/nm)				emission max (λ/nm)		RLS
	OHPP	422	519	556	595	651	657	721	
Cl^-	H_2OHPP^{2+} [a]	450							
	$H_2OHPP^{2+}_{agg}$	490			691	775			512
Br^-	H_2OHPP^{2+a}	455							
	$H_2OHPP2+_{agg}$	473			655	724			512
I^-	H_2OHPP^{2+} [a]	454							
	$H_2OHPP^{2+}_{agg}$	494			654	732			517
	$HOHPP^+_{dim}$ [a]	427					610	655	
CF_3COO^-	$H_2OHPP^{2+}_{agg}$	480			671	642			499
	H_2OHPP^{2+}	449			630	687		738	
$CF_3SO_3^-$	$H_2OHPP^{2+}_{agg}$	503				727			505
	H_2OHPP^{2+}	452			613	677	685	719	
$TFPB^-$	H_2OHPP^{2+}	454			606	689	684	741	

[a] Intermediate species.

consisting in the detection of the intermediate monomeric diacids in all cases. Also OHPP aggregates ($\{H_2OHPP(X)_2\}_{agg}$, X = Cl, Br, I) display extremely broad extinction features, whose positions follow the trend observed for THPP (see Tables 1 and 2).

Red-shifted and broad extinction bands are quite common for aggregated porphyrins,[30,31,40−45] especially due to the presence of resonant light scattering components near the absorption bands.[46,47] To explain the extinction features observed for THPP and OHPP aggregates, a consideration of both their hyperporphyrin character[2,12−15] and aggregation phenomena is required.

In the attempt of proposing a model for the interaction of the porphyrins in the aggregates, a J-type arrangement of the monomers can be proposed on the basis of the red shift ($\Delta\lambda \sim +40$ nm) of the aggregate extinction bands with respect to the monomeric diacid intermediate. A distorted porphyrin macrocycle has been suggested considering the large amount of structural details, both experimental and theoretical, present in the literature on the saddling of the porphyrin plane upon core diprotonation.[29,48−54] These studies, together with the observed dependence of the spectral properties of THPP and OHPP aggregates on the nature of the halide, allow one to assume the presence of strong interactions between the protonated porphyrin core and the various counteranions, as suggested for TpyP isomers and TPPS.[30,31] In fact, the stabilization of the aggregates structure may be achieved through a network of electrostatic interactions and hydrogen bonding between the protonated core and the peripheral hydroxyl groups, mediated by the halide anions (Figure 3; model for $\{H_2THPP(X)_2\}_{agg}$, X = Cl, Br, I). On one hand, the formation of extended hydrogen-bonding networks has been observed in the solid-state structures of free base porphyrins bearing hydroxyphenyl *meso*-substituents.[55−58] On the other hand, the proposed model is further supported by a recent analysis performed via DFT and TDDFT calculations on the diacid derivatives of tetraphenylporphyrin ($\{H_2TPP(X)_2\}$, X = F, Cl, Br, I).[29] This study shows that a strong interaction is present between the halides and the protonated N−H groups of this diacid and that, besides electrostatics, covalent interactions are a relevant component in the total energy of this hydrogen bond.

TMPP displays a quite different behavior with respect to the other two porphyrins under study. As observed for TPP solutions in dichloromethane,[29] the addition of HCl vapors to TMPP leads to the formation of its monomeric diacid derivative. The spectral changes accompanying the conversion from the free base to

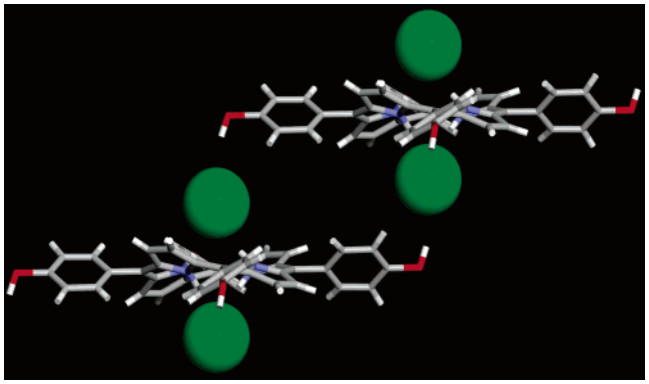

Figure 3. Side view of the proposed model for the J-aggregation of $\{H_2THPP(X)_2\}$ through the intermediacy of halide anions, shown as green spheres (charges omitted for clarity).

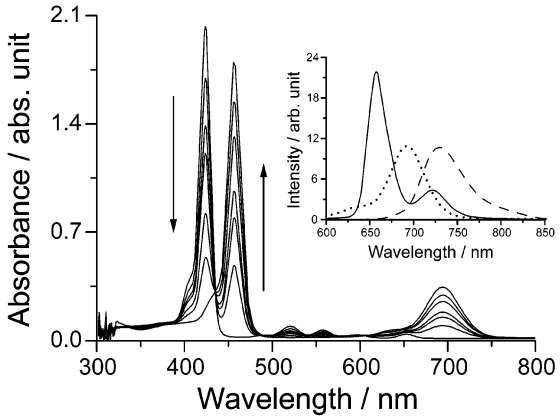

Figure 4. UV/vis spectral changes following the stepwise addition of HCl to a dichloromethane solution of TMPP ([TMPP] = 4.6 μM). Arrows mark the evolution due to the increase of acid concentration (up to ~100 μM). Inset: Fluorescence spectra of starting (solid line) and acidified (dashed) solutions. Dotted line: Q-bands of $\{H_2THPP(Cl)_2\}$.

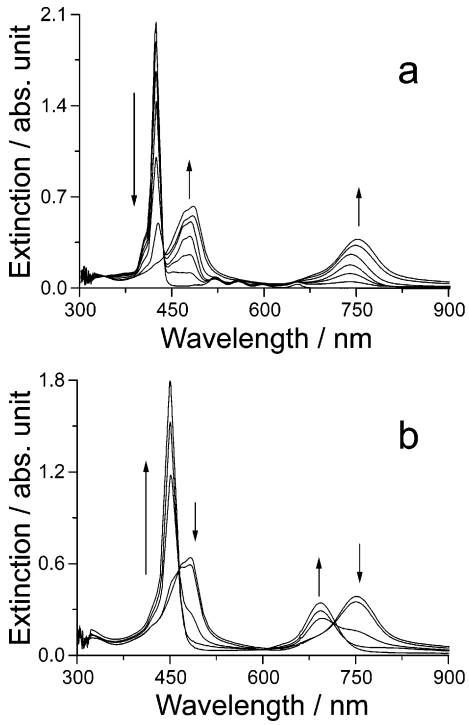

Figure 5. UV/vis spectral changes following the stepwise addition of CF_3COOH to a dichloromethane solution of THPP ([THPP] = 4.6 μM). Arrows mark the evolution due to the increase of acid concentration (a, up to ~170 μM; b, up to ~20 mM). Key: (a) from THPP to $\{H_2THPP(X)_2\}_{agg}$; (b) from $\{H_2THPP(X)_2\}_{agg}$ to $\{H_2THPP(X)_2\}$ (X = CF_3COO).

the diacid species are reported in Figure 4, with the occurrence of several isosbestic points. The new Soret band is red-shifted with respect to that of the starting compound, and the number of the Q-bands is reduced from 4 to 2 as a consequence of the change in molecular symmetry (from D_{2h} to D_{2d}). Also the fluorescence is strongly affected by core diprotonation, displaying red-shifted emission (Stokes shift: 628 cm^{-1}; Figure 4, inset) with a reduced intensity. No enhancement of resonance light scattering is observed in the acidified solutions, consistent with the putative monomeric nature of the diacid derivative ($\{H_2TMPP(Cl)_2\}$).

The same behavior is observed on adding other acids (HX, X = Br, I, CF_3COO, CF_3SO_3) to TMPP solutions, and a dependence of the spectroscopic features of the various diacid derivatives on the nature of the counteranion is evident also for this porphyrin (see Table 3). This dependence suggests the presence of ion-pairing interactions between diprotonated porphyrin core and counteranions, with the likely formation of tight ion pairs due to the low dielectric constant of dichloromethane.

Considering the three halide derivatives, the Soret band of $\{H_2TMPP(I)_2\}$ exhibits the strongest hypochromic effect, and fluorescence intensity follows the order $\{H_2TMPP(Cl)_2\}$ > $\{H_2TMPP(Br)_2\}$ > $\{H_2TMPP(I)_2\}$, as reported for the TPP system.[29] TMPP diacids derived from the two oxygen-containing acids (CF_3COOH and CF_3SO_3H) display smaller bathochromic shifts of the Soret band with respect to the starting free base, and their emission intensities are comparable to that of the chloride derivative.

The absence of aggregation phenomena in the case of TMPP highlights the role of peripheral hydroxyl groups in the interaction among the monomeric units in the aggregates. The presence of methoxy groups, instead of the four hydroxyl substituents of THPP, prevents the formation of hydrogen bonds between the protonated porphyrin core of a monomer and the periphery of a neighboring one, impeding aggregation (through the intermediacy of anions).

Acidification experiments carried out on THPP and OHPP solutions with CF_3COOH or CF_3SO_3H display a common pattern of behavior, illustrated in Figure 5 by the THPP/CF_3COOH system. Two steps can be identified during the experiment, consisting of initial aggregation phenomena followed by aggregate disruption. At first, the extinction spectral changes upon acid addition show the conversion of the sharp Soret band of THPP free base to a broad, red-shifted feature which seems to be constituted of at least two components (Figure 5a). The intensities of the Q-bands (considerably red-shifted) are comparable to the corresponding B-band, and their number is reduced to 2. At this stage the system is extensively aggregated, as indicated by complete quenching of the fluorescence and by the presence of a very intense RLS signal (Figure 6, green lines). On continued acid additions, the broad Soret band converts into a sharper

TABLE 3: UV/Vis Absorption, Emission, and RLS Features of Species Derived from Porphyrin TMPP in the Presence of Various Acids HX in Dichloromethane at 298 K

X^-	species	B-band (λ/nm)	Q-bands (λ/nm)				emission max (λ/nm)		RLS
	TMPP	422	519	556	595	651	657	721	
Cl^-	H_2TMPP^{2+}	454			633	692		730	
Br^-	H_2TMPP^{2+}	458			633	692		736	
I^-	H_2TMPP^{2+}	456			646	707		747[a]	
CF_3COO^-	H_2TMPP^{2+}	451			629	687		732	
$CF_3SO_3^-$	H_2TMPP^{2+}	452			627	689		733	
$TFPB^-$	H_2TMPP^{2+}	456			637	700		747	

[a] Very weak

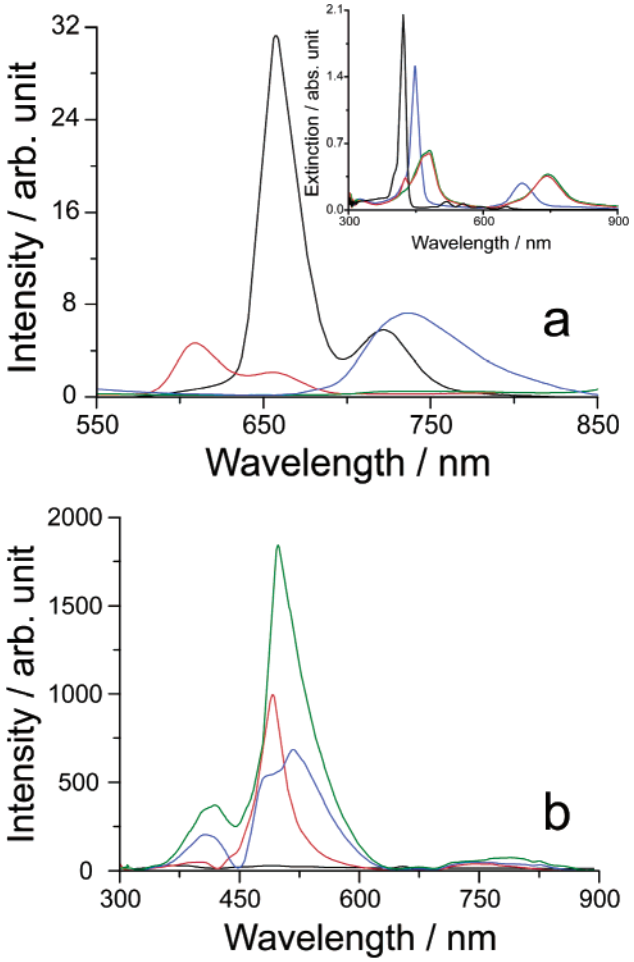

Figure 6. Fluorescence emission (a), extinction (a, inset), and RLS (b) spectra of the various species obtained by adding CF_3COOH to a dichloromethane solution of THPP ([THPP] = 4.6 μM): THPP (black lines); $\{H_2THPP(X)_2\}_{agg}$ (X = CF_3COO, green lines); $\{H_2THPP(X)_2\}$ (blue lines). Red lines belong to the intermediate species (see text).

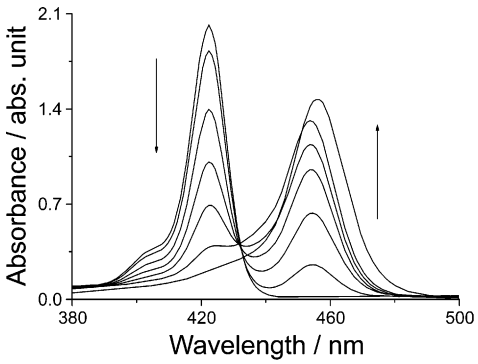

Figure 7. UV/vis spectral changes following the stepwise addition of HTFPB to a dichloromethane solution of TMPP ([TMPP] = 4.6 μM). Arrows mark the evolution due to the increase of acid concentration (up to ~250 μM).

feature centered at 448 nm, and the Q-bands shift to the blue (Figure 5b). At the end of this second step the fluorescence spectrum displays a broad emission band and the resonant light scattering signal is reduced (Figure 6, blue lines). These observations are consistent with partial aggregate disruption in favor of the formation of monomeric diacid species, probably due to the rise of the environment polarity as the CF_3COOH concentration increases. Before the end of the first step is attained, the

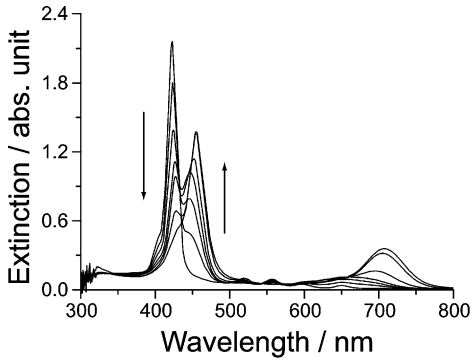

Figure 8. UV/vis spectral changes following the stepwise addition of HTFPB to a dichloromethane solution of THPP ([THPP] = 4.9 μM). Arrows mark the evolution due to the increase of acid concentration (up to ~450 μM).

SCHEME 1: Observed Pattern of Behavior for Protonation/Aggregation of the Three Tetraarylporphyrins (TMPP, THPP, OHPP) with Various HX in Dichloromethane[a]

$$\{(H_2TArP^{2+})\cdot(X^-)_2\} \quad (1)$$

$$TArP \xrightarrow{+HX} \{(H_2TArP^{2+})\cdot(X^-)_2\}_{agg} \quad (2)$$

$$\{(H_2TArP^{2+})\cdot(X^-)_2\}_{agg} \xrightarrow{+HX} \{(H_2TArP^{2+})\cdot(X^-)_2\} \quad (3)$$

[a] See Table 4.

TABLE 4: Pattern of Behavior for the Various Systems Described in Scheme 1

acid	TMPP	THPP	OHPP
HCl	1	2	2
HBr	1	2	2
HI	1	2	2
CF_3COOH	1	3[a]	3[a]
CF_3SO_3H	1	3	3
HTFPB	1	1[b]	2

[a] An intermediate species is detected in the conversion from free base to aggregate. [b] An intermediate species is detected in the conversion from free base to diacid.

existence of an intermediate species is revealed by exciting the fluorescence emission of the sample at 427 nm (Figure 6, red lines; observed also with OHPP). If the position of the B-band of the intermediate species (427 nm) is regarded as resulting from a blue shift of the monomeric diacid Soret band (448 nm), the intermediate may be considered as an H-dimer of diprotonated porphyrins.

The three porphyrins differ from each other in their behavior toward acidification with tetrakis[3,5-bis(trifluoromethyl)phenyl]-boric acid (HTFPB). This acid has been chosen for the low coordinating ability of its anion which, in the case of TpyP isomers, allowed us to isolate species with an intermediate degree of protonation.[30] The isosbestic points usually observed in the spectral changes occurring along with the acidification experiments involving TMPP are not observed with this acid, especially upon the last additions. Initially, the Soret band of the acidified species appears at 454 nm and is accompanied by two Q-bands at 636 and 693 nm. At the end of the experiment both B- and Q-bands are slightly red-shifted ($\Delta\lambda = +2$ and $+1$ and $+7$ nm, respectively; Figure 7). The lack of isosbestic points is more evident for the THPP/HTFPB system (Figure 8), pointing to the formation of an intermediate species in the

conversion of the free base into the diacid derivative. No aggregation phenomena are observed throughout this acidification experiment; thus, the intermediate species may be tentatively assigned to a porphyrin monoprotonated at the core, even if ion-pairing or hydrogen-bonding interactions involving phenolyc OH groups and HTFPB cannot be excluded a priori. Differently, on addition of HTFPB acid to OHPP solutions, formation of aggregates is indicated by the presence of strong RLS signals. The dissimilarity between TMPP and THPP can be explained considering the inductive effects of the four methoxy groups on the peripheral *meso*-substituents, which cause the first porphyrin to be a stronger base than THPP.[59] The aggregation of OHPP can be rationalized considering the presence of four additional hydroxyl groups with respect to THPP, which give rise to supplementary hydrogen-bonding interactions thus favoring the formation of aggregates.[55−58]

The possibility to obtain monoacid species of *meso*-aryl porphyrins on HTFPB additions can be related to the properties of the bulky $TFPB^-$ anion. Experiments carried out on TpyP(4) with this same acid show that the interaction between the protonated porphyrin macrocycle and the counteranions is relevant for the proton transfer to occur.[30] In the peripherally protonated $\{H_4TpyP(4)(TFPB)_4\}$, the four encumbering anions are ion-paired with the protonated pyridyl groups and hinder the approach of a fifth $TFPB^-$ anion, preventing or consistently reducing also the proton transfer. The noncoordinating character of $TFPB^-$, together with its steric demand, may be the explanation for the observation of supposed monoacid porphyrin intermediates in the case of THPP.

Concluding Remarks

The behavior toward acidification of TMPP, THPP, and OHPP in dichloromethane solutions has been studied as a function of the nature of the acid, and it is summarized in Scheme 1, with Table 4 identifying the various patterns of behavior displayed by the different porphyrin/acid systems.

In the presence of various acids, TMPP yields monomeric diacid derivatives, like TPP, while aggregation phenomena have been observed with the two porphyrins bearing hydroxyphenyl substituents. These groups allow the occurrence of noncovalent interactions between neighboring monomeric units of diacid species, stabilizing aggregate formation.[55−58]

The possibility of modulating the optical properties of such hyperporphyrins aggregates by changing the nature of the counteranion gives access to supramolecular noncovalent dye systems with potential optical application in the near-infrared portion of the electromagnetic spectrum.

Acknowledgment. The authors thank the MIUR (COFIN 2004) for financial support.

References and Notes

(1) Hambright, P. Chemistry of water soluble porphyrins. In *The Porphyrin Handbook*; Kadish, K. M., Smith, K. M., Guilard, R., Eds.; Academic Press: New York, 2000; Vol. 3, p 129.

(2) Gouterman, M. In *The Porphyrins*; Dolphin, D., Ed.; Academic Press: New York, 1978; Vol. 3, p 1.

(3) Bonnett, R. *Chem. Soc. Rev.* **1995**, *24*, 19.

(4) Lang, K.; Mosinger, J.; Wagnerova, D. M. *Coord. Chem. Rev.* **2004**, *248*, 321.

(5) Sharman, W. M.; Allen, C. M.; van Lier, J. E. *Drug Discovery Today* **1999**, *4*, 507.

(6) Bonnett, R.; White, R. D.; Winfield, U. J.; Berenbaum, M. C. *Biochem. J.* **1989**, *261*, 277.

(7) Neta, P.; Richoux, M. C.; Harriman, A.; Milgrom, L. R. *J. Chem. Soc., Faraday Trans. 2* **1986**, *82*, 209.

(8) Bonnett, R.; McGarvey, D. J.; Harriman, A.; Land, E. J.; Truscott, T. G.; Winfield, U. J. *Photochem. Photobiol.* **1988**, *48*, 271.

(9) Bonnett, R.; Martinez, G. *Org. Lett.* **2002**, *4*, 2013.

(10) Ojadi, E. C. A.; Linschitz, H.; Gouterman, M.; Walter, R. I.; Lindsey, J. S.; Wagner, R. W.; Droupadi, P. R.; Wang, W. *J. Phys. Chem.* **1993**, *97*, 13192.

(11) Vitasovic, M.; Gouterman, M.; Linschitz, H. *J. Porphyrins Phthalocyanines* **2001**, *5*, 191.

(12) Wasbotten, I. H.; Conradie, J.; Ghosh, A. *J. Phys. Chem. B* **2003**, *107*, 3613.

(13) Weinkauf, J. R.; Cooper, S. W.; Schweiger, A.; Wamser, C. C. *J. Phys. Chem. A* **2003**, *107*, 3486.

(14) Guo, H.; Jiang, J.; Shi, Y.; Wang, Y.; Liu, J.; Dong, S. *J. Phys. Chem. B* **2004**, *108*, 10185.

(15) Guo, H.; Jiang, J.; Shi, Y.; Wang, Y.; Dong, S. *J. Phys. Chem. B* **2006**, *110*, 587.

(16) Lindsey, J. S.; Delaney, J. K.; Mauzerall, D. C.; Linschitz, H. J. *J. Am. Chem. Soc.* **1988**, *110*, 3610.

(17) Gouterman, M.; Wagniere, G. H.; Snyder, L. C. *J. Mol. Spectrosc.* **1963**, *11*, 108.

(18) Hanson, L. K.; Eaton, W. A.; Sligar, S. G.; Gunsalus, I. C.; Gouterman, M.; Connell, C. R. *J. Am. Chem. Soc.* **1976**, *98*, 2672.

(19) Sono, M.; Andersson, L. A.; Dawson, J. H. *J. Biol. Chem.* **1982**, *257*, 8308.

(20) Dawson, J. H.; Andersson, L. A.; Sono, M. *J. Biol. Chem.* **1983**, *258*, 13637.

(21) Stern, J. O.; Peisach, J. *J. Biol. Chem.* **1974**, *249*, 7495.

(22) Chang, C. K.; Dolphin, D. *J. Am. Chem. Soc.* **1976**, *98*, 1607.

(23) Ruf, H. H.; Wende, P. *J. Am. Chem. Soc.* **1977**, *99*, 5499.

(24) Sakurai, H.; Ishizu, K. *J. Am. Chem. Soc.* **1982**, *104*, 4960.

(25) Doppelt, P.; Fischer, J.; Weiss, R. *J. Am. Chem. Soc.* **1984**, *106*, 5188.

(26) Daeid, N. N.; Atkinson, S. T.; Nolan, K. B. *Pure Appl. Chem.* **1993**, *65*, 1541.

(27) Sakurai, H.; Tamura, J.; Yoshimura, T. *Inorg. Chem.* **1985**, *24*, 4227.

(28) Sakurai, H.; Uchikubo, H.; Ishizu, K.; Tajima, K.; Aoyama, Y.; Ogoshi, H. *Inorg. Chem.* **1988**, *27*, 2691.

(29) Rosa, A.; Ricciardi, G.; Baerends, E. J.; Romeo, A.; Scolaro, L. M. *J. Phys. Chem. A* **2003**, *107*, 11468.

(30) De Luca, G.; Romeo, A.; Scolaro, L. M. *J. Phys. Chem. B* **2005**, *109*, 7149.

(31) De Luca, G.; Romeo, A.; Scolaro, L. M. *J. Phys. Chem. B* **2006**, *110*, 7309.

(32) De Luca, G.; Pollicino, G.; Romeo, A.; Scolaro, L. M. *Chem. Mater.* **2006**, *18*, 2005.

(33) Scolaro, L. M.; Romeo, A.; Castriciano, M. A.; De Luca, G.; Patane, S.; Micali, N. *J. Am. Chem. Soc.* **2003**, *125*, 2040.

(34) Pasternack, R. F.; Collings, P. J. *Science* **1995**, *269*, 935.

(35) Adler, A. D.; Longo, F. R.; Finarelli, J. D.; Goldmacher, J.; Assour, J.; Korsakoff, L. *J. Org. Chem.* **1967**, *32*, 476.

(36) Bonar-Law, R. P. *J. Org. Chem.* **1996**, *61*, 3623.

(37) A higher methanol concentration does not allow the formation of aggregates on acid addition, probably for the corresponding increase of the dielectric constant of the solvents mixture.

(38) Brookhart, M.; Grant, B.; Volpe, A. F. *Organometallics* **1992**, *11*, 3920.

(39) Simplified symbol for $\{(H_2TMPP^{2+})(Cl^-)_2\}$. Hereafter, this notation will be used to represent ion pairs, unless otherwise specified.

(40) Pasternack, R. F.; Goldsmith, J. I.; Szep, S.; Gibbs, E. J. *Biophys. J.* **1998**, *75*, 1024.

(41) Purrello, R.; Bellacchio, E.; Gurrieri, S.; Lauceri, R.; Raudino, A.; Scolaro, L. M.; Santoro, A. M. *J. Phys. Chem. B* **1998**, *102*, 8852.

(42) Gurrieri, S.; Aliffi, A.; Bellacchio, E.; Lauceri, R.; Purrello, R. *Inorg. Chim. Acta* **1999**, *286*, 121.

(43) Pasternack, R. F.; Ewen, S.; Rao, A.; Meyer, A. S.; Freedman, M. A.; Collings, P. J.; Frey, S. L.; Ranen, M. C.; de Paula, J. C. *Inorg. Chim. Acta* **2001**, *317*, 59.

(44) De Napoli, M.; Nardis, S.; Paolesse, R.; Vicente, M. G. H.; Lauceri, R.; Purrello, R. *J. Am. Chem. Soc.* **2004**, *126*, 5934.

(45) Scolaro, L. M.; Romeo, A.; Castriciano, M. A.; Micali, N. *Chem. Commun.* **2005**, 3018.

(46) Micali, N.; Mallamace, F.; Castriciano, M.; Romeo, A.; Scolaro, L. M. *Anal. Chem.* **2001**, *73*, 4958.

(47) Collings, P. J.; Gibbs, E. J.; Starr, T. E.; Vafek, O.; Yee, C.; Pomerance, L. A.; Pasternack, R. F. *J. Phys. Chem. B* **1999**, *103*, 8474.

(48) Barkigia, K. M.; Fajer, J.; Berber, M. D.; Smith, K. M. *Acta Crystallogr., Sect. C: Cryst. Struct. Commun.* **1995**, *C51*, 511.

(49) Stone, A.; Fleischer, E. B. *J. Am. Chem. Soc.* **1968**, *90*, 2735.

(50) Senge, M. O. *Chem. Commun. (Cambridge, U.K.)* **2006**, 243.

(51) Juillard, S.; Ferrand, Y.; Simonneaux, G.; Toupet, L. *Tetrahedron* **2005**, *61*, 3489.

(52) Cheng, B.; Munro, O. Q.; Marques, H. M.; Scheidt, W. R. *J. Am. Chem. Soc.* **1997**, *119*, 10732.

(53) Rosa, A.; Ricciardi, G.; Baerends, E. J. *J. Phys. Chem. A* **2006**, *110*, 5180.

(54) Chirvony, V. S.; van Hoek, A.; Galievsky, V. A.; Sazanovich, I. V.; Schaafsma, T. J.; Holten, D. *J. Phys. Chem. B* **2000**, *104*, 9909.

(55) Bhyrappa, P.; Wilson, S. R.; Suslick, K. S. *J. Am. Chem. Soc.* **1997**, *119*, 8492.

(56) Bhyrappa, P.; Wilson, S. R.; Suslick, K. S. *Supramol. Chem.* **1998**, *9*, 169.

(57) Goldberg, I.; Krupitsky, H.; Stein, Z.; Hsiou, Y.; Strouse, C. E. *Supramol. Chem.* **1994**, *4*, 203.

(58) Suslick, K. S.; Bhyrappa, P.; Chou, J.-H.; Kosal, M. E.; Nakagaki, S.; Smithenry, D. W.; Wilson, S. R. *Acc. Chem. Res.* **2005**, *38*, 283.

(59) Meot-Ner, M.; Adler, A. D. *J. Am. Chem. Soc.* **1975**, *97*, 5107.